

# Photometry and Spectroscopy of a Deep Algol-like Minimum of WW Vulpeculae in 2016

David Boyd

West Challow Observatory, OX12 9TX, UK; davidboyd@orion.me.uk

Received July 29, 2024; revised August 19, 2024; accepted August 20, 2024

**Abstract** We report analysis of photometry and spectroscopy of a deep Algol-like minimum of the pre-main-sequence star WW Vul in July and August 2016. This revealed substantial reddening due to absorption by circumstellar material. After dereddening, our spectra of WW Vul were consistent with spectral type A3V throughout the event. H $\alpha$  is normally in emission in WW Vul. During the minimum, H $\alpha$  emission dropped by  $\sim 30\%$  and FWHM of the H $\alpha$  line reduced by  $\sim 15\%$ .

## 1. Background on WW Vul

WW Vulpeculae was included in a list of RW Aurigae stars published by Hoffmeister in 1949. These are photometrically variable stars not assigned to any particular class. It was also included in the ‘‘Second Supplement to the Mount Wilson Catalogue’’ of stars with spectral types B and A whose objective-prism spectra have bright hydrogen emission (Merrill and Burwell 1949). Herbig (1960) compiled a list of 26 stars with spectral type Ae or Be associated with nebulosity and having emission lines in their spectra which he suggested were in the process of contracting onto the main sequence. These stars have come to be known as Herbig Ae/Be (or HAeBe) stars. Herbig’s conjecture that HAeBe stars were young pre-main-sequence stars was confirmed by Strom *et al.* (1972), who showed that they are pre-main-sequence stars surrounded by optically thick circumstellar shells of dust which are possibly disc-like. Over the following years many authors discussed the nature of HAeBe stars and WW Vul in particular, including among others Grinin *et al.* (1996), Grinin *et al.* (2001), Hernandez *et al.* (2004), Mendigutia *et al.* (2011), and references therein. WW Vul is also described as an UXOR star, a term invented by Herbst *et al.* (1994) to classify young variable stars with masses in the approximate range 2 to 8  $M_{\odot}$  and strong H $\alpha$  emission lines whose variability characteristics are similar to those of the prototype UX Ori.

A consensus has emerged that these stars are surrounded by a protoplanetary disc-like envelope seen almost edge-on containing optically thick clouds which orbit the star within the disc. Material accretes from the cloud onto the young star. Variable obscuration by these clouds causes irregular changes and occasional deep Algol-like minima in their light curves. According to this model the star’s brightest state represents its intrinsic luminosity. The circumstellar material contains larger dust grains than occur in the interstellar medium and these strongly redden light emerging from the star. H $\alpha$  emission lines in the spectrum of these stars originate not in the stellar photosphere but in the circumstellar gas and a stellar wind.

By comparison with spectra of standard stars, Merrill and Burwell (1949) gave the spectral type of WW Vul as A3e, Mora *et al.* (2001) classified its spectral type as A2IVe, and Hernandez *et al.* (2004) used an extensive range of spectral features to assign spectral type A3 with an uncertainty of  $\pm 2$  subtypes.

For the purpose of our analysis, we will take the spectral type of WW Vul to be A3V. Fitzgerald (1970) gave the intrinsic color index  $(B-V)_0$  of an A3V star as 0.08, while Pecaut and Mamajek (2013) gave  $(B-V)_0 = 0.10$ . We will adopt 0.09. By analysis of spectral lines in comparison with synthetic spectra, Mora *et al.* (2004) estimated the photospheric effective temperature of WW Vul as 9000 K, Hernandez *et al.* (2004) gave 8710 K, and Pecaut and Mamajek (2013) gave the effective temperature of an A3V star as 8600 K. Hernandez *et al.* (2004) gave the mass of WW Vul as 2.9  $M_{\odot}$ , while Mendigutia *et al.* (2011) gave 2.5  $M_{\odot}$ .

## 2. Observations

Examining the long-term AAVSO light curve of WW Vul (AAVSO 2024) shows that it experiences long periods when its magnitude varies by less than 0.5 magnitude, interrupted by aperiodic Algol-like minima up to 2 magnitudes deep. Only twice in the last 20 years, in 2016 and 2019, has the V magnitude of WW Vul been repeatedly recorded fainter than 12. Here we analyze the deep minimum of WW Vul in July and August 2016 which reached V magnitude 12.12.

Photometric observations were made at West Challow Observatory in Oxfordshire in the UK with a 0.35-m Schmidt-Cassegrain telescope and Astrodon B and V photometric filters. Images were bias, dark, and flat corrected and instrumental magnitudes obtained by aperture photometry using the software AIP4WIN (Berry and Burnell 2005). A weighted ensemble of five nearby comparison stars was used whose B and V magnitudes and errors were obtained from AAVSO Variable Star Chart X27286KL (AAVSO 2016). Instrumental B and V magnitudes were transformed to the Johnson UBV photometric standard using the measured  $(B-V)$  color index and atmospheric airmass for each image. Times were recorded as Julian Date (JD).

B and V magnitudes and  $(B-V)$  color indices recorded before, during, and after the deep minimum in 2016 are listed in Table 1 and plotted in Figure 1. The  $(B-V)$  color index of WW Vul became redder as it faded before levelling out at minimum as shown in Figure 2. During the fade, the V-band flux of WW Vul dropped by  $\sim 75\%$ . Recovery from minimum had an irregular profile, suggesting opacity of the material causing obscuration was changing from day to day.

Spectroscopic images were obtained concurrently with the photometry at the same location with a 0.28-m Schmidt-

Cassegrain telescope and a LISA slit spectrograph (Shelyak Instr. 2024) with spectral resolving power of  $\sim 1000$ . Images were bias, dark, and flat corrected, geometrically corrected, sky background subtracted, 1D spectrum extracted, and finally wavelength calibrated using the integrated argon-neon calibration source. Each WW Vul spectrum was corrected for instrumental and atmospheric losses by recording the spectrum of a nearby star from the MILES library of stellar spectra (Falc3n-Barroso *et al.* 2011) observed at an airmass close to WW Vul. A list of recorded spectra is given in Table 2.

By recording photometry and spectroscopy concurrently, we were able to use the V magnitudes to calibrate all our spectra in absolute flux in units of  $\text{erg}/\text{cm}^2/\text{sec}/\text{\AA}$  using the method described in Boyd (2020). All photometry and spectra were submitted to, and are available from, the BAA Photometry Database and the BAA Spectroscopy Database (BAA 2024a, 2024b), respectively.

### 3. Circumstellar extinction and dereddening

Taking the intrinsic color index  $(B-V)_0$  of WW Vul as 0.09, we found the color excess  $E(B-V)$  for each of our spectra from  $E(B-V) = (B-V) - (B-V)_0$ . These  $E(B-V)$  values are listed in Table 2. As selective extinction by circumstellar dust increased, it caused the star to fade, to redden, and  $E(B-V)$  to increase.

Gaia DR3 (Bailer-Jones *et al.* 2021) gave the distance of WW Vul as  $480 \pm 4$  pc. At this distance it is unlikely that the star will have experienced much galactic interstellar extinction.  $R_V$  is the ratio of total visual extinction  $A(V)$  to selective extinction  $E(B-V)$ . Hernandez *et al.* (2004) found that visual extinction measured for 39 HAeBe stars within 1 kpc including WW Vul is consistent with  $R_V = 5.0$  rather than the usually adopted value of 3.1 for mean galactic interstellar extinction. They concluded that the high level of extinction for these stars is most likely produced by a combination of circumstellar material close to the star and material from their associated molecular clouds.

This circumstellar material reddens photospheric emission from WW Vul and changes the slope of the continuum. In our flux-calibrated spectra, WW Vul appeared to be closest to spectral type F2V from the Pickles atlas (Pickles 1998). To find its intrinsic spectral type we had to deredden our spectra. To do this we adopted  $R_V = 5.0$  and used the relationships in Cardelli *et al.* (1989) to calculate  $A(\lambda)/A(V)$  for each spectrum with the appropriate value of  $E(B-V)$  from Table 2. We applied this wavelength-dependent dereddening to each of our spectra. Figure 3 shows examples of our flux-calibrated spectra before and after dereddening and identifies some of the absorption lines in the spectra.

We compared each of our dereddened spectra of WW Vul with A2V, A3V, and A4V spectra from the Pickles atlas. These have similar resolution to our spectra. Of these, A3V gave the most consistent match to all our spectra, in agreement with published results. Figure 4 shows two dereddened spectra of WW Vul, one taken before the fade and one at minimum, together with Pickles A3V spectra.

Table 1. Log of B and V magnitudes and  $(B-V)$  color indices recorded before, during and after the deep minimum in 2016.

Date	JD	B (mag)	V (mag)	$(B-V)$ (mag)
03-Jul-2016	2457573.4745	10.69	10.38	0.32
13-Jul-2016	2457583.4546	10.81	10.45	0.36
17-Jul-2016	2457587.5037	10.90	10.55	0.35
22-Jul-2016	2457592.4758	10.79	10.47	0.32
23-Jul-2016	2457593.4455	10.76	10.44	0.33
28-Jul-2016	2457598.4214	10.85	10.51	0.34
05-Aug-2016	2457606.4113	11.10	10.70	0.40
08-Aug-2016	2457609.4122	11.55	11.06	0.49
09-Aug-2016	2457610.3887	11.85	11.32	0.53
09-Aug-2016	2457610.4192	11.86	11.34	0.53
11-Aug-2016	2457612.4592	12.67	12.12	0.55
13-Aug-2016	2457614.4157	11.90	11.36	0.54
14-Aug-2016	2457615.3976	12.27	11.71	0.56
15-Aug-2016	2457616.4231	11.94	11.39	0.55
16-Aug-2016	2457617.4820	11.72	11.20	0.52
18-Aug-2016	2457619.3639	11.76	11.25	0.52
19-Aug-2016	2457620.3705	11.80	11.30	0.50
22-Aug-2016	2457623.3906	11.30	10.86	0.44
23-Aug-2016	2457624.3707	11.16	10.75	0.41
26-Aug-2016	2457627.3938	10.98	10.60	0.38
30-Aug-2016	2457631.3637	10.87	10.52	0.35
31-Aug-2016	2457632.4334	10.84	10.49	0.35
11-Sep-2016	2457643.3562	10.84	10.52	0.32
22-Sep-2016	2457654.3663	10.90	10.54	0.36

Note: Average uncertainties in B are 0.014, in V are 0.012 and in  $B-V$  are 0.019.

Table 2. Log of spectroscopic observations of WW Vul during the deep minimum in 2016 with color excess and integrated  $H\alpha$  emission line flux.

Date	JD	$E(B-V)$	$H\alpha$ emission line flux ( $\text{erg}/\text{cm}^2/\text{sec}$ )
17-Jul-2016	2457587.5037	0.26	2.13E-12
23-Jul-2016	2457593.4455	0.24	2.08E-12
05-Aug-2016	2457606.4113	0.31	1.48E-12
08-Aug-2016	2457609.4122	0.40	1.41E-12
09-Aug-2016	2457610.3887	0.44	1.35E-12
11-Aug-2016	2457612.4592	0.46	1.32E-12
14-Aug-2016	2457615.3976	0.47	1.34E-12
15-Aug-2016	2457616.4231	0.46	1.33E-12
16-Aug-2016	2457617.4820	0.43	1.28E-12
22-Aug-2016	2457623.3906	0.35	1.73E-12
26-Aug-2016	2457627.3938	0.29	1.75E-12
11-Sep-2016	2457643.3562	0.23	1.82E-12

Note: The estimated uncertainty in line flux is 15%.

### 4. $H\alpha$ emission

Figures 3 and 4 show that our spectra of WW Vul have the broad Balmer absorption lines expected in a normal A3V star but with a narrower emission peak within the  $H\alpha$  absorption. This emission has been attributed to photospheric emission causing excitation in the circumstellar material and stellar wind. As the star faded, the  $H\alpha$  absorption dip weakened while the emission component remained strong. Figure 4 shows a small emission feature also appeared within the  $H\beta$  absorption line at minimum.

To measure absolute flux in the  $H\alpha$  emission line, we first scaled the Pickles A3V spectrum to match the flux level of the

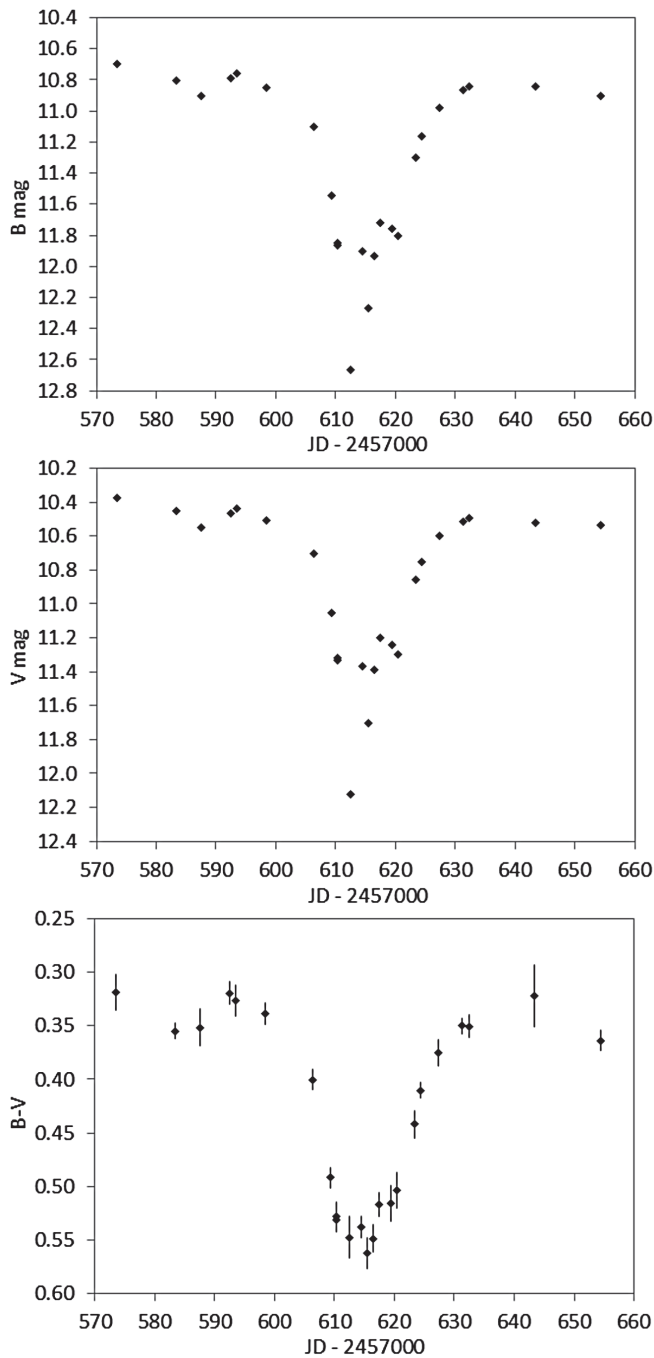


Figure 1. Variation of B and V magnitudes and (B–V) color index before, during, and after the deep minimum of WW Vul in 2016.

continuum adjacent to the  $H\alpha$  line in each of our dereddened WW Vul spectra and binned it to match the resolution of our spectra. We subtracted this from each of our WW Vul spectra to give the  $H\alpha$  emission flux in excess of photospheric emission. We then integrated this flux over the wavelengths of the line to give the total flux in the  $H\alpha$  line in that spectrum in  $\text{erg}/\text{cm}^2/\text{sec}$ . These data are listed in Table 2. The uncertainty in  $H\alpha$  flux is a combination of the uncertainties in determining the continuum level outside the line and in measuring the flux in the line.

Previous analyses of  $H\alpha$  emission (e.g. Mendigutia *et al.* 2011) have usually been in terms of equivalent width since, in general, the absolute flux in their spectra was not known.

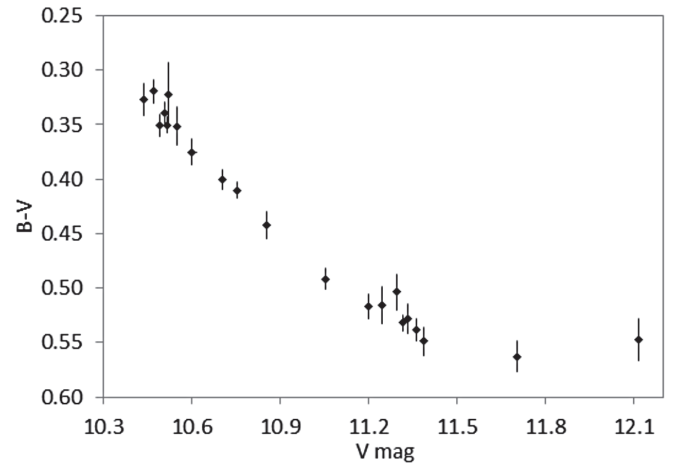


Figure 2. Variation of (B–V) color index as V magnitude faded.

By flux-calibrating our spectra, we were able to measure the strength of  $H\alpha$  emission in absolute flux. Figure 5 shows how flux in the continuum at  $H\alpha$ ,  $H\alpha$  equivalent width, and  $H\alpha$  emission flux varied during the deep minimum in 2016.  $H\alpha$  equivalent width increased by a factor of three during the fade but because the continuum simultaneously decreased,  $H\alpha$  emission flux actually reduced by  $\sim 30\%$  compared to its mean value before and after the event. This indicates that the source of  $H\alpha$  emission is partially blocked by the circumstellar material causing the fade.

Figure 6 shows the changing profile of the  $H\alpha$  emission line before, during, and after the fade. Before and after the fade the line was double-peaked, suggestive of a rotating circumstellar disc seen edge-on, while at minimum it became single-peaked. To investigate whether the width of the line varied during the fade, we fitted the emission peak with a Gaussian profile. Although the lines were sometimes double-peaked, a Gaussian profile fitted the rising and falling edges of all the lines well and so gave an accurate measurement of their full width at half maximum (FWHM). These FWHM measurements are plotted in Figure 7 and show that the  $H\alpha$  line became  $\sim 15\%$  narrower during the fade. The Gaussian fits also gave the central wavelength of each line. These showed the lines were systematically displaced by  $0.3 \pm 0.3 \text{ \AA}$  towards the blue with respect to the rest wavelength of the line. Unfortunately there is no radial velocity for WW Vul available in Gaia DR3.

Figure 8 is a composite plot using color coding to illustrate the correlation between changes in spectral flux with wavelength and time in the upper panel and the variation in V magnitude with time in the left panel during the 2016 minimum of WW Vul. The red dots in the left panel mark the times of the spectra in the upper panel. The flux in the lower right panel is color-coded in  $\text{ergs}/\text{cm}^2/\text{sec}/\text{\AA}$  according to the color scale on the right, with color linearly interpolated between the spectral profiles in the upper panel. This 2D color-coded plot provides a way of visualising the correlation between changes in spectral flux, V magnitude, and time that is not provided by separate plots of each parameter.

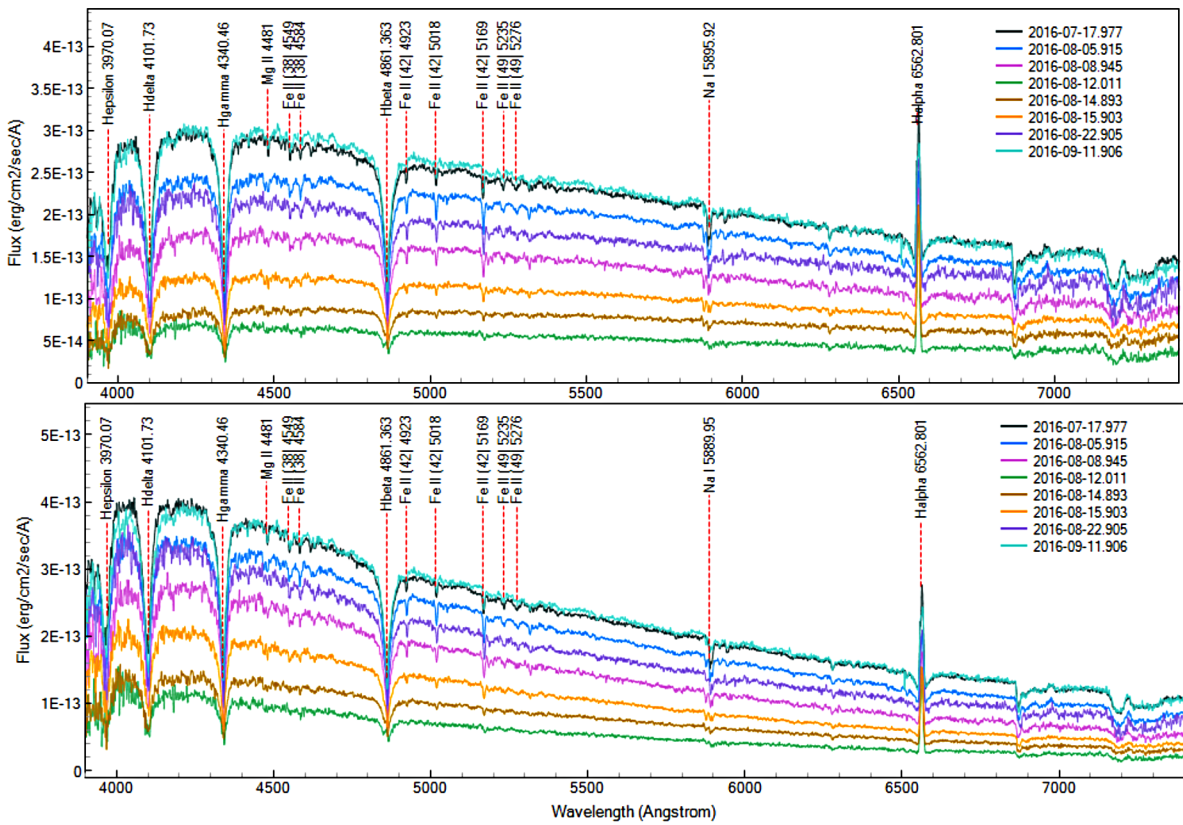


Figure 3. Examples of flux-calibrated spectra of WW Vul before (upper) and after (lower) dereddening, with identification of some of the absorption lines.

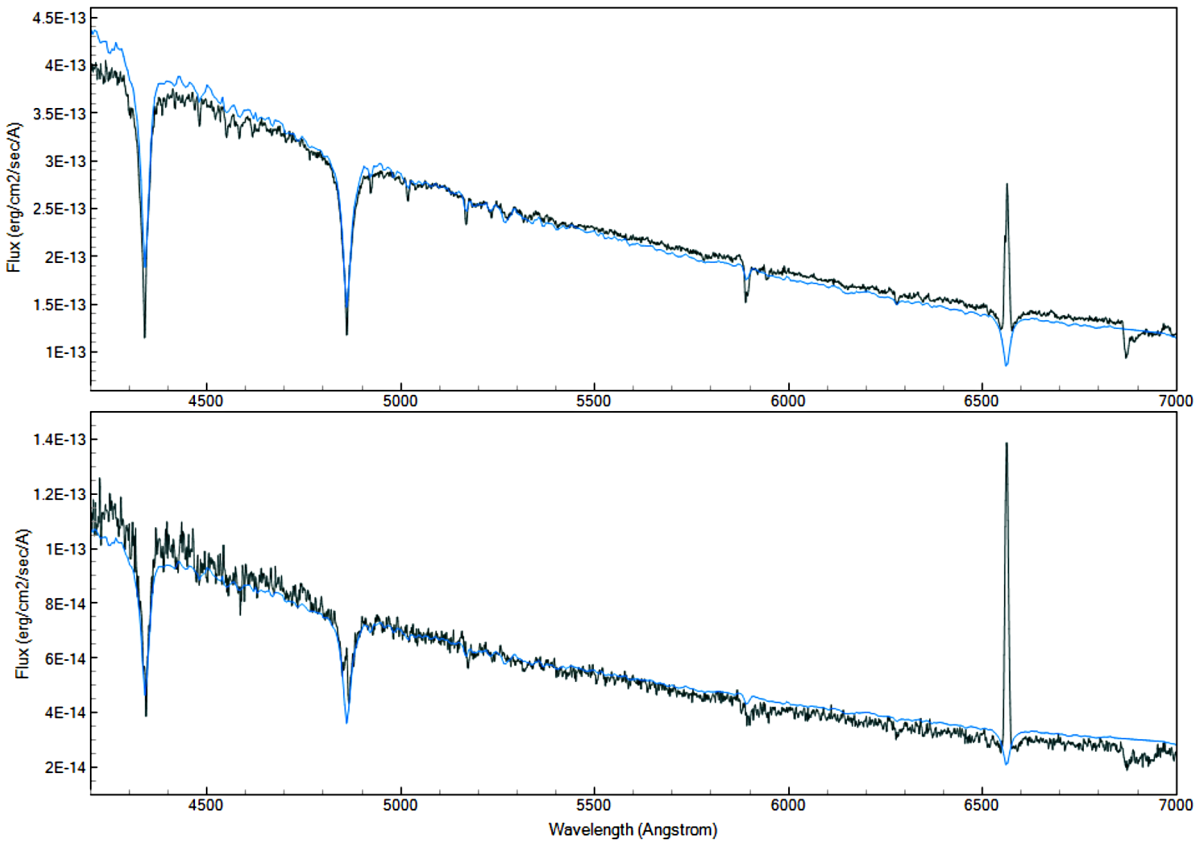


Figure 4. Comparing two dereddened spectra of WW Vul, one taken before the fade (upper) and one at minimum (lower), both with an A3V spectrum from the Pickles atlas (Pickles 1998).

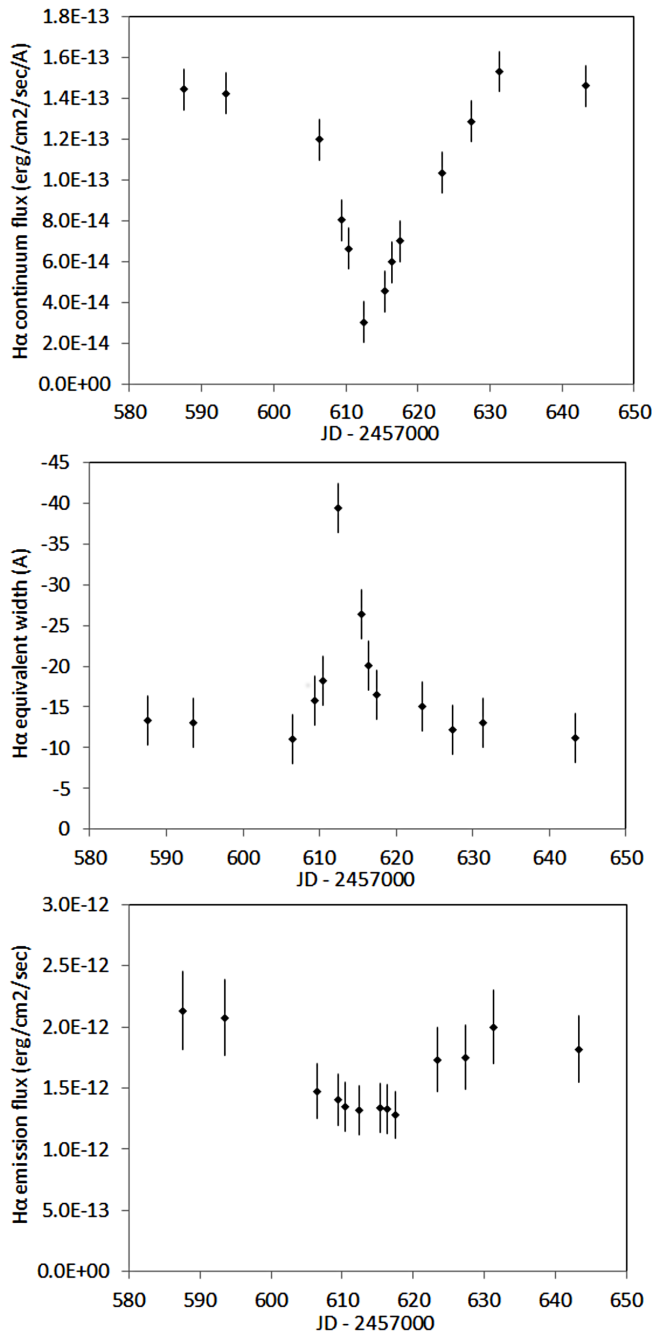


Figure 5. Continuum flux, equivalent width, and emission flux at H $\alpha$  before, during, and after the deep minimum of WW Vul in 2016.

**5. Summary**

We observed a deep minimum of the pre-main-sequence star WW Vul in July and August 2016 with concurrent B- and V-band photometry and low resolution spectroscopy. We observed behavior consistent with the general consensus that transient obscuration by dense clouds of circumstellar dust in our line of sight substantially reduces direct photospheric emission and changes the slope of the continuum. We observed a  $\sim 75\%$  drop in V-band flux of WW Vul and progressive reddening during the fade. We used our V-band photometry to flux calibrate our spectra and our measured values of  $E(B-V)$  to deredden our spectra. We found that the spectral type of WW Vul after

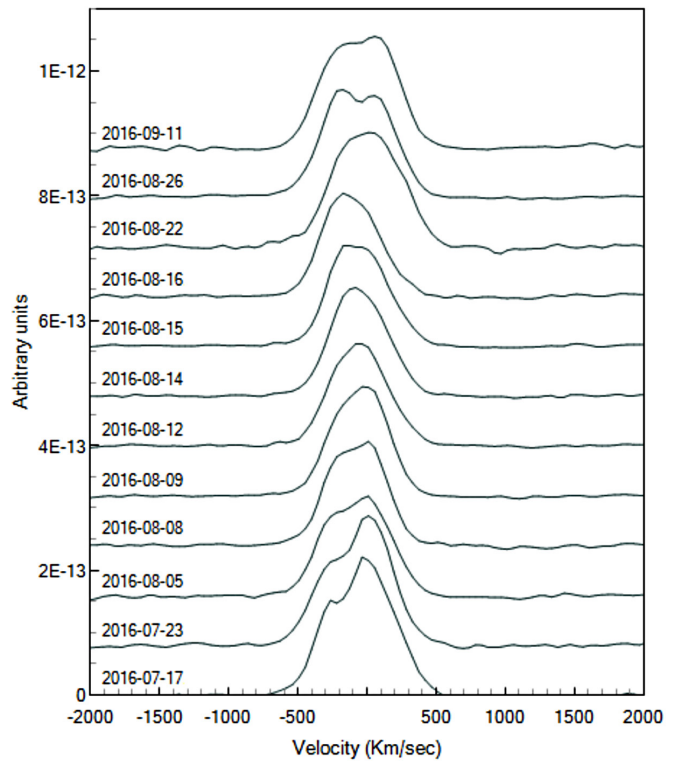


Figure 6. H $\alpha$  emission line profile in spectra recorded during the 2016 minimum of WW Vul showing the line was double peaked before and after the fade but became single peaked at minimum.

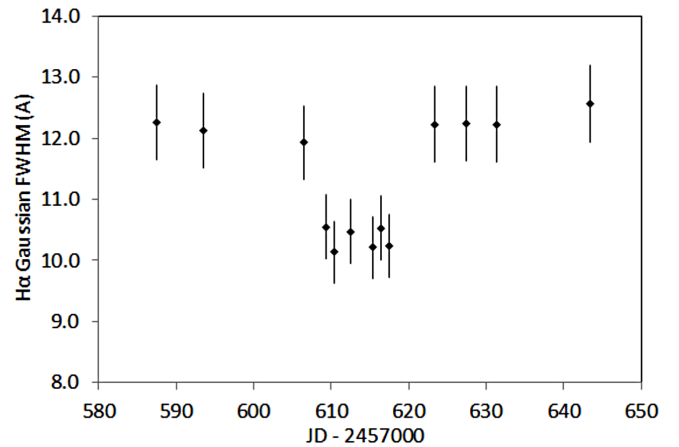


Figure 7. FWHM of Gaussian fits to H $\alpha$  emission lines before, during, and after the 2016 minimum of WW Vul.

dereddening consistently matched spectral type A3V throughout the fade. We measured the H $\alpha$  emission lines and found their flux dropped by  $\sim 30\%$  and their FWHM reduced by  $\sim 15\%$  during the fade. The profile of the H $\alpha$  line was double-peaked before and after the fade but became single-peaked at minimum.

**6. Acknowledgements**

We are grateful to the referee for a constructive review which helped us improve the paper. We also acknowledge the use of AAVSO Variable Star Charts and the work of developers of the Astropy package and other contributors to this valuable community resource.

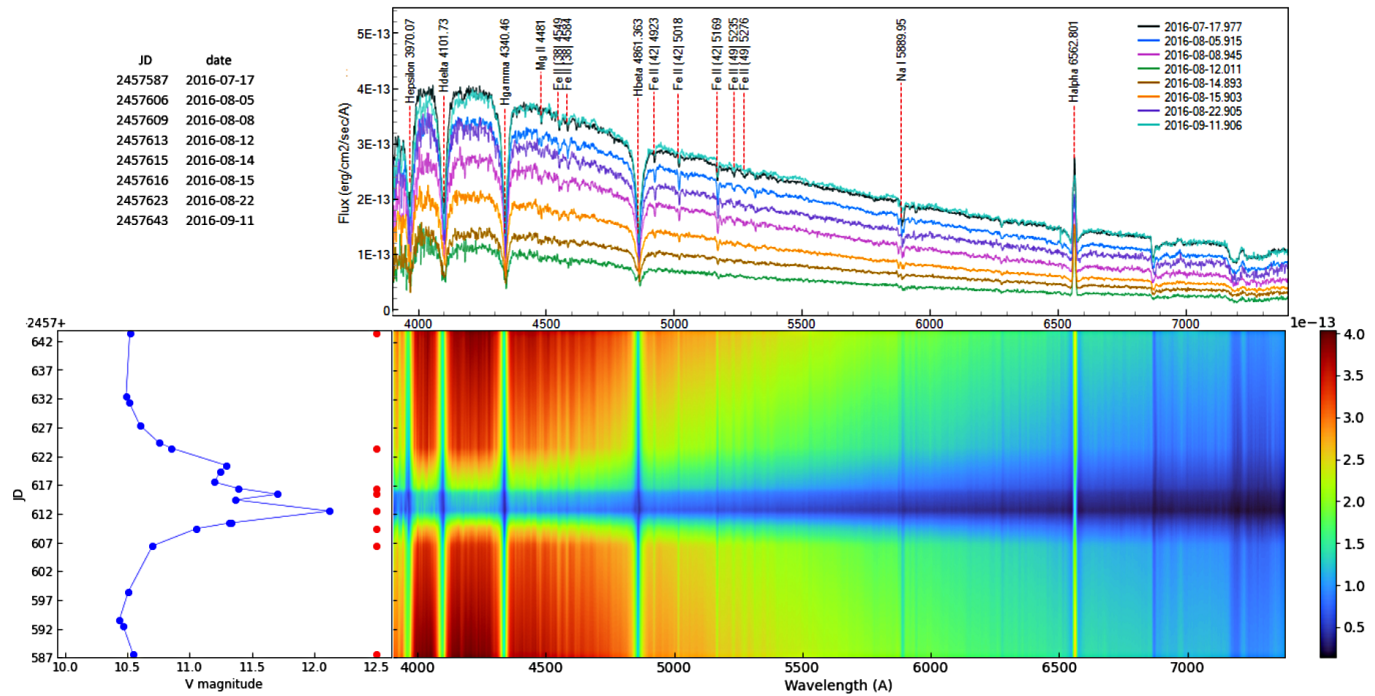


Figure 8. Composite plot using color coding to illustrate the correlation between changes in spectral flux with wavelength and time in the upper panel and the variation in V magnitude with time in the left panel during the 2016 minimum of WW Vul. The red dots in the left panel mark the times of the spectra in the upper panel. The flux in the lower right panel is color-coded in ergs/cm<sup>2</sup>/sec/Å according to the color scale on the right with color linearly interpolated between the spectral profiles in the upper panel.

## References

- AAVSO. 2016, AAVSO Variable Star Plotter (VSP; <https://www.aavso.org/apps/vsp>).
- AAVSO. 2024, AAVSO Light Curve Generator (LCGv2), WW Vul long-term light curve.<sup>1</sup>
- Bailer-Jones, C. A. L., Rybizki, J., Fouesneau, M., Demleitner, M., and Andrae, R. 2021, *Astron. J.*, **161**, 147.
- Berry, R., and Burnell, J. 2005, *Handbook of Astronomical Image Processing*, Willmann-Bell, Richmond, VA.
- Boyd, D. 2020, “A method of calibrating spectra in absolute flux using V magnitudes.” (<https://britastro.org/sites/default/files/absfluxcalibration.pdf>).
- British Astronomical Association. 2024a, BAA Photometry Database (<https://britastro.org/photdb>).
- British Astronomical Association. 2024b, BAA Spectroscopy Database (<https://britastro.org/specdb>).
- Cardelli, J. A., Clayton, G. C., and Mathis, J. S. 1989, *Astrophys. J.*, **345**, 245.
- Falcón-Barroso, J., Sánchez-Blázquez, P., Vazdekis, A., Ricciardelli, E., Cardiel, N., Cenarro, A. J., Gorgas, J., and Peletier, R. F. 2011, *Astron. Astrophys.*, **532A**, 95.
- Fitzgerald, M. P. 1970, *Astron. Astrophys.*, **4**, 234.
- Grinin, V. P., Kozlova, O. V., Natta, A., Ilyin, I., Tuominen, I., Rostopchina, A. N., and Shakhovskoy, D. N. 2001, *Astron. Astrophys.*, **379**, 482.
- Grinin, V. P., Kozlova, O. V., The, P. S., and Rostopchina, A. N. 1996, *Astron. Astrophys.*, **309**, 474.
- Herbig G. H. 1960, *Astrophys. J., Suppl. Ser.*, **4**, 337.
- Herbst, W., Herbst, D. K., Grossman, E. J., and Weinstein, D. 1994, *Astron. J.*, **108**, 1906.
- Hernández, J., Calvet, Nn, Briceño, C., Hartmann, L., and Berlind, P. 2004, *Astron. J.*, **127**, 1682.
- Hoffmeister, C. 1949, *Astron. Nachr.*, **278**, 24.
- Mendigutía, I., Eiroa, C., Montesinos, B., Mora, A., Oudmajer, R. D., Merín, B., and Meeus, G. 2011, *Astron. Astrophys.*, **529A**, 34.
- Merrill, P. W., and Burwell, C. G. 1949, *Astrophys. J.*, **110**, 387.
- Mora, A., et al. 2001, *Astron. Astrophys.*, **378**, 116.
- Mora, A., et al. 2004, *Astron. Astrophys.*, **419**, 225.
- Pecaut, M. J., and Mamajek, E. E. 2013, *Astrophys. J., Suppl. Ser.*, **208**, 9.
- Pickles, A. J. 1998, *Publ. Astron. Soc. Pacific*, **110**, 863.
- Shelyak Instruments. 2024, LISA Spectroscop (VIS). <https://www.shelyak.com/produit/spectroscopie-lisa-vis/?lang=en>
- Strom, S. E., Strom, K. M., Yost, J., Carrasco, L., and Grasdalen, G. 1972, *Astrophys. J.*, **173**, 353.

<sup>1</sup> AAVSO (2024),

<https://www.aavso.org/LCGv2/index.htm?DateFormat=Julian&RequestedBands=&view=api.delim&ident=WW%20Vul&fromjd=460490&tojd=2460660&delimiter=@@@>